THE MUTUAL EFFECT OF PRECIPITATED AURORAL ELECTRONS AND THE AURORAL ELECTROJET*

by

Bernt N. Maehlum and Brian J. O'Brien

Department of Space Science
Rice University
Houston, Texas

GPO PRICE $ _____
CFSTI PRICE(S) $ _____
Hard copy (HC) 3.00
Microfiche (MF) .65
ff 653 July 65

To be presented at the IUGG General Assembly, St. Gall, Switzerland, September 1967.

*Research supported in part by the National Aeronautics and Space Administration under Contract NAS6-1061 and Grant NsG-673.

FACILITY FORM 602
N68-25713 (ACCESSION NUMBER) (THRU)
18 (PAGES) 1 (CODE)
NASA CR OR TMX OR AD NUMBER) 13 (CATEGORY)

THE MUTUAL EFFECT OF PRECIPITATED AURORAL ELECTRONS AND THE AURORAL ELECTROJET

by

Bernt N. Maehlum and Brian J. O'Brien

Department of Space Science
Rice University
Houston, Texas

Abstract. It has been found that the perturbation in the geomagnetic field produced by the auroral electrojet also perturbes the pitch angle distribution of the precipitated electrons which are the dominant contributors to the auroral ionization within which it is assumed the auroral electrojet flows. In order to study this interaction in detail a computer program has been developed for model calculations. This program computes:

(1) the electron density profile in the ionosphere from a given pitch angle and energy distribution of the ionizing electrons, and

(2) the changes in the pitch angle distribution created by the geomagnetic field deformations caused by the auroral electrojet current system itself.

Results from preliminary computations are discussed. It is shown that the interaction can cause significant time variations in an initially time-stationary electron precipitation event. Thus, for the first time it is seen that naturally occurring atmospheric "feed-back" effects can account for some of the dynamic auroral variations without requiring the auroral source itself to vary in time. The variations are governed by the pitch angle distribution and the total flux of precipitated electrons as well as by the normal loss parameters in the upper atmosphere. For medium to strong electron precipitation events the calculated periodicity of the variations lies in the range of 50 to 200 seconds, which is in agreement with some of the direct observations of auroral electron periodicities.

INTRODUCTION

The existence of horizontal, mainly East - West flowing currents in the auroral ionosphere has been known for many years, although the mechanisms involved in the production and maintenance of these currents are still uncertain [Chapman and Bartels, 1940; Bostrom, 1964; Axford and Hines, 1961; Fejer, 1963]. It is generally believed that the time variations in the current are caused partly by variations in the driving electric field, partly by variations in the ionospheric conductivity. Although it has not been proven, the currents are believed to be located close to visual auroral forms, which indicates that precipitating energetic electrons are the main sources of the ionization associated with the enhanced conductivity in the electric current.

Recently, Cummings, et al.[1966] drew attention to the fact the the geomagnetic field distortion caused by the currents may modify the pitch angle distribution of the precipitated electrons, which in its turn will affect the electron density in the ionosphere. Theoretical studies of the effects of the auroral current on the electron pitch angle distribution and vice versa have been continued at Rice University, and we present here a few results from these studies.

We will show that the variations in the geomagnetic field caused by the auroral electrojet (whose intensity is dominated by the ionization produced by the precipitated electrons) can in turn modulate the pitch angle distribution of these precipitated electrons and thence in a cyclic repetitive form modulate the electrojet and thence the precipitated particles. The ultimate consequence is development of a natural periodicity of oscillation of both the auroral ionization and of the precipitation of the particles themselves.

METHOD OF COMPUTATION

In the computations to be discussed it was assumed that the shape of the energy spectrum and the pitch angle distribution of the precipitated electrons at a reference altitude (1000 km) are constant in a latitude interval $\Delta\lambda$, and the spectrum was assumed to obey an exponential law with e-folding energy E_o = 5 keV, having a low-energy cut-off at 2.5 keV, independent of pitch angle. Outside this latitude interval the fluxes are zero, and all parameters are assumed constant in the East - West direction. In order to compute rapidly the energy dissipation of the electrons in the atmosphere, the altitude variations in the geomagnetic field in the current region (100 - 140 km) were neglected, but the variation of the field in latitude due to the presence of the current was taken into account exactly. By using Alfven's invariant and Liouville's theorem the pitch-angle distribution of the precipitated electrons at 140 km was deduced from the distribution at 1000 km. The ionization rates in the ionosphere due to the precipitated electrons were obtained by integrating the contributions from all electron pitch angles, using data from electron-scatter computations [Stadsnes and Maehlum, 1967]. The electron-density profile was computed by assuming a recombination-like loss of ionization:

$$\frac{dN_e}{dt} = \frac{q}{1+\lambda} - \alpha N_e^2 \qquad (1)$$

where the "effective" recombination coefficient α and the negative ion-to-electron density ratio λ were interpolated from data given by Holt [1964] and Yonezawa [1962] for auroral conditions. (In the actual height interval between 100 and 140 km $\alpha \approx 10^{-7}$ cm^3/sec and $\lambda \approx 0$). The initial "background" electron density was assumed to be negligible with respect to the auroral ionization.

The current-driving electric field was obtained by assuming a given distortion in the horizontal component of the geomagnetic field (ΔB_{Hor}) on the ground. It is not known how the driving electric field varies with the electron density, and we have as a first-order approximation assumed that the current density is proportional to the electron density. Earth-induced currents were assumed to contribute $\sim$ 40% to ΔB_{Hor}.

The distortion of the geomagnetic field was computed by summing up the contributions from all parts of the current. The resultant distortion in the pitch-angle distribution of the precipitating electrons could then be deduced, and the time variations in the auroral current were computed by going through this loop repeatedly. The integration step was selected to be much shorter than the time constant of the ionosphere as deduced from Equation (1). Although various attempts have been made to save computing time, each integration step takes 1 - 2 minutes on an IBM 7040 computer. A few preliminary results from the calculations are presented in the following sections. In all our computations the current is flowing toward the West and the latitude parameter runs from North to South.

Spatial Variations in the Ionospheric Electron Density Caused by Current-Induced Geomagnetic Field Distortions.

The series of computations clearly demonstrate that a very complicated relationship exists between the electron precipitation and the auroral current system, and it is very difficult to select models of computation which are "typical" for actual auroral events.

Let us first consider the following simple case: the electron precipitation is assumed constant over a 10-km-wide latitude interval at 1000 km, and the pitch-angle distribution of the electron fluxes above 40 keV at 1000 km is as indicated

as A in Figure 1. The current produced by the electron precipitation is assumed to give a geomagnetic disturbance $\Delta B_{Hor} = -1000\gamma$. The latitude variations in the peak, equilibrium ionization at 110 km altitude caused by this flux of precipitated electrons is shown in Figure 2.

The latitude variation of the ionization depends critically on the pitch angle distribution of electrons in the "loss cone". This is seen by comparing the curves labeled A and B in Figures 1 and 2.

For a very sharply defined loss cone (C in Figure 1) an interesting effect occurs. Close to the northern boundary (X = 0 km) the distorted geomagnetic field intensity will be sufficiently high to prevent the electrons from reaching the atmosphere. Therefore, after a short period of "build-up" of ionization the electron density starts to decrease in the northern part of the current region. During a strong disturbance ($\Delta B_{Hor} = -1000\gamma$) this particular electron pitch angle distribution is not able to establish a time stationary auroral current, because the electron density oscillates. These oscillations, which are discussed in more detail in the next section, only occur during strong geomagnetic disturbances. If similar computations are performed for the same configuration of electron precipitation (C in Figure 1) for a smaller geomagnetic disturbance ($\Delta B_{Hor} = -250\gamma$), no oscillations occur, but it is interesting to note that the latitude variations in the equilibrium electron density is very large, and there are even some indications of a fine-scale structure inside the region of precipitation (see curve C', Figure 2).

Time Variations in the Electron Precipitation Caused by Particle-Ionosphere Interaction.

Pulsations in auroral zone phenomena have been observed recently from ground-based, rocket and balloon experiments. The

periods reported vary from 0.2 secs [Anderson and Milton, 1964] to about 200 secs [Barcus and Rosenberg, 1965]. Various mechanisms have been suggested for different types of pulsations, but very little is yet known of the sources of the modulations. In the past, it has always been assumed that these modulations were due to modulations of the primeval source mechanisms. By contrast, in the present section we discuss the periods of oscillations produced by low-altitude interaction between electron fluxes and the auroral currents. Furthermore, we discuss what electron pitch angle distributions and geomagnetic disturbances are required for causing oscillations in the precipitations. For simplicity, we will only be concerned with pitch angle distributions with a sharply defined "loss cone".

The series of computations performed refer to the following configuration of electron precipitation: the pitch angle distribution of electrons at 1000 km altitude is assumed isotropic between 90° and an angle α_c, (α_c can vary between 48° and 58°), and for pitch angles between 0° and α_c the fluxes are assumed to be zero. The precipitation is restricted to a latitude interval of 20 km, inside which the fluxes vary by a factor of ~ 20 (see Figure 3). This is meant to simulate an actual event with high electron fluxes embedded in a low background flux.

In the first example we selected a value of $\alpha_c = 54^{\circ}$, which is slightly less than the quiet day "loss cone" boundary, and the average, horizontal geomagnetic disturbance on the ground was $\Delta B_{Hor} \approx -600\gamma$. Results from the computations are given in Figures 4 and 5.

The total electron energy precipitated per second into a vertical column of the atmosphere with 1 cm^2 cross section is shown in a contour plot in Figure 4 as a function of time and latitude. Similarly, the variations in the geomagnetic field at 110 km altitude are indicated in Figure 5.

During the first few seconds after the onset of the particle flux there is a gradual increase in the ion production at all latitudes. This is accompanied by an enhancement in the ionospheric current, which increases the geomagnetic field near the northern boundary of the region of precipitation. This geomagnetic field enhancement will cause the electrons to mirror above the scattering region, and the ion production is very small in this region. As the electron density and therefore the current gradually decreases in the northern part up to t = 60 secs the geomagnetic field returns to a normal value, and a new "burst" of ionization occurs near t = 90 secs as electrons again are allowed to penetrate into the atmosphere. After this time similar bursts occur every 90 to 100 seconds periodically. Near the southern boundary the electrons are "guided" into the atmosphere due to the decreased geomagnetic field. Therefore, a strong current builds up near the southern boundary.

An energy flux of ~ 1 erg/cm^2 sec (for the energy spectrum discussed in this paper) produces an equilibrium ionospheric layer with a peak electron density of $\sim 3.10^5$cm^{-3} [Brown, 1964]. The electron density corresponding to the "event" shown in Figure 4 varied between 2.10^5 and 3.10^6cm^{-3}.

Similar computations for other electron fluxes show the same general type of pattern. When the fluxes of electrons above 40 keV are 10^5 - 10^6#/cm^{2}sec sterad, the period of oscillation is 200 - 250 seconds, whereas a period of $\sim$ 10 - 15 secs occurs when the ionizing electron fluxes are as high as 10^8 - 10^9#/cm^{2}sec sterad. Such high fluxes have very infrequently been observed [O'Brien and Laughlin, 1962]. We therefore conclude that long period oscillations may occur in the auroral phenomena due to particle-atmosphere interactions if the current driving electric field is sufficiently strong and the gradient in the pitch angle distribution of the ionizing electrons is

steep near the boundary of the "loss cone". The period of pulsations caused by this interaction is in the 50 - 300 seconds range for reasonable fluxes of ionizing electrons.

A summary of some of the model computations is presented in Figure 6 to show how the equilibrium conditions vary with the effective "cut-off" angle in the electron pitch angle distribution and with geomagnetic activity. The broken lines refer to cases when oscillations occurred, whereas the short, continuous lines correspond to time-stationary distributions. From this figure we conclude that oscillations in the precipitated electron fluxes due to ionospheric "feed-back" can occur during very disturbed geomagnetic conditions only, unless the loss cone is extremely well defined. The stability does not seem to depend on the intensity of precipitation (directional fluxes of greater than 40 keV energies for the various cases computed are indicated by small numbers in Figure 6).

Long-period oscillations have been observed in the auroral X-rays [Barcus and Rosenberg, 1965] and in the visual aurora [Omholt and Berger, 1967]. Both phenomena occur during geomagnetically disturbed conditions after midnight and in the morning hours. With our present lack of knowledge on the diurnal variations in the electron pitch angle distribution we are not in a position to evaluate the importance of the ionospheric "feed-back" as contributor to these pulsations. Synoptic satellite and rocket experiments of electron pitch angle distributions and geomagnetic field distortions are needed for solving this problem. Further computations are being performed for a variety of the numerous parameters.

CONCLUDING COMMENTS

One of the greatest mysteries in the studies of auroral morphology and of the electron fluxes that apparently accompany auroras has been the temporal fluctuations in both of these phenomena. In the past it has often been assumed, and indeed it has generally been assumed, that these temporal fluctuations are a reflection of corresponding fluctuations in the primeval particle fluxes themselves and that consequently they may have deep seated implications as regards the unknown source of the energetic electrons that cause auroras. By contrast we have shown in this paper that it is extremely important to consider the fact that the atmosphere and the ionosphere play a critical role in the dynamic morphology of auroras and electron precipitation events. Indeed while the fundamental electron source may remain uniform in time at altitudes above 1000 km one can still have periodic or pulsating variations both in particle precipitation and in the consequent auroral morphology and ionospheric ionization simply due to what one might call an inevitable interaction or atmospheric feedback upon the particle fluxes themselves.

Acknowledgements: This research was supported in part by the National Aeronautics and Space Administration under Contract NAS6-1061 and Grant NsG-673.

REFERENCES

Anderson, K. A. and D. W. Milton, J. Geophys. Res., 69, 4457, 1964.

Axford, W. I., and C. O. Hines, Canad. J. Phys., 39, 1433, 1961.

Barcus, J. R. and T. J. Rosenberg, J. Geophys. Res., 70, 1707, 1965.

Bostrom, R., J. Geophys. Res., 69, 1983, 1964.

Brown, R. R., Ark. Geofysik, 4, 405, 1964.

Chapman, S. and J. Bartels, "Geomagnetism", Oxford University Press, 1940.

Cummings, W. D., R. E. LaQuey, B. J. O'Brien and M. Walt, J. Geophys. Res., 71, 1399, 1966.

Fejer, J. A., J. Geophys. Res., 68, 2147, 1963.

Holt, O., N.D.R.E. Report No. 46, Norwegian Defence Res. Est., Kjeller, Norway, 1963.

O'Brien, B. J., and C. D. Laughlin, J. Geophys. Res., 67, 2667, 1962.

Omholt, A. and S. Berger, Planet. Space Sci., 15, 1075, 1965.

Stadnes, J. and B. Maehlum, Intern Rapport No. 54, Norwegian Defence Res. Est., Kjeller, Norway, 1965.

Yonezawa, T., In "Electron Density Profiles", ed. by B. Maehlum, Pergamon Press, 1962.

FIGURE CAPTIONS

Figure 1: Model pitch angle distributions of integral electron flux above 40 keV energy at 1000 km altitude.

Figure 2: Latitude profile of the equilibrium peak electron density produced by the precipitated electron fluxes shown in Figure 1. [Geomagnetic field distortions on the ground are indicated in brackets].

Figure 3: Latitudinal variations in the integral electron fluxes above 40 keV energy for pitch angle of 90^{o} at 1000 km altitude.

Figure 4: Time and spatial variations in the total precipitated electron energy flux into the atmosphere for 1000-km input of 50 - 1000 ergs/cm^2sec (See text).

Figure 5: Time and spatial variations in the geomagnetic field at 110 km altitude (See text).

Figure 6: Stability of the electron precipitation during various degrees of geomagnetic disturbance (Directional fluxes of electrons for pitch angles greater than α_c are indicated with small lettering).

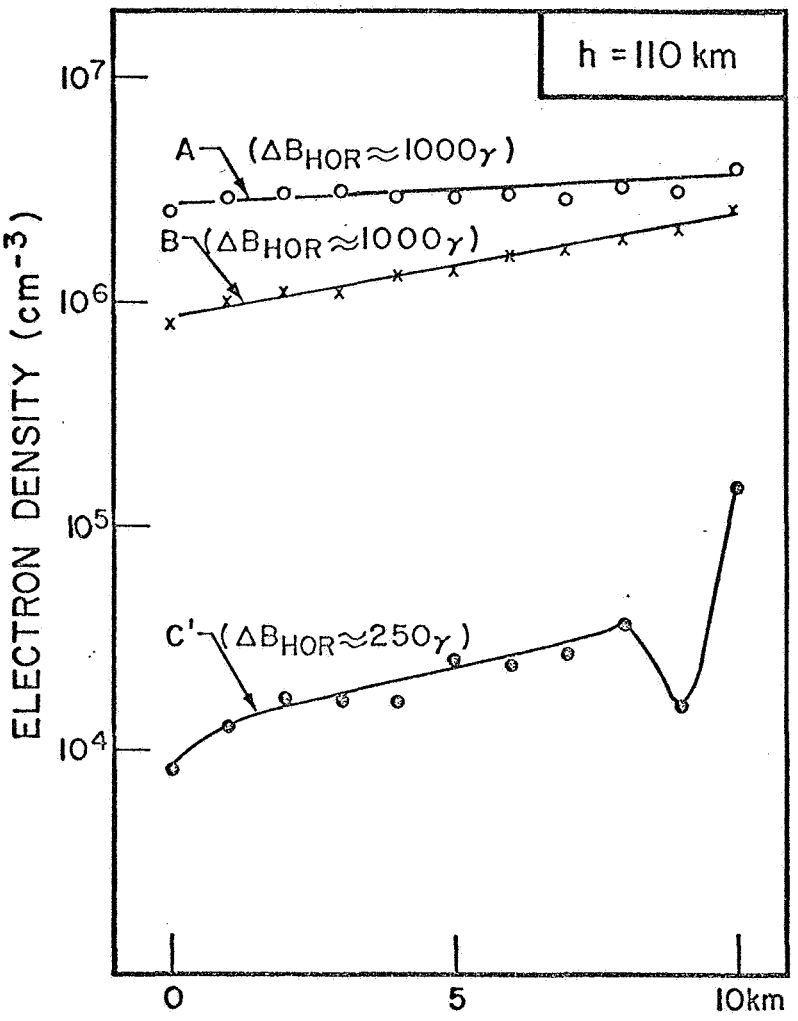

Figure 1

201309

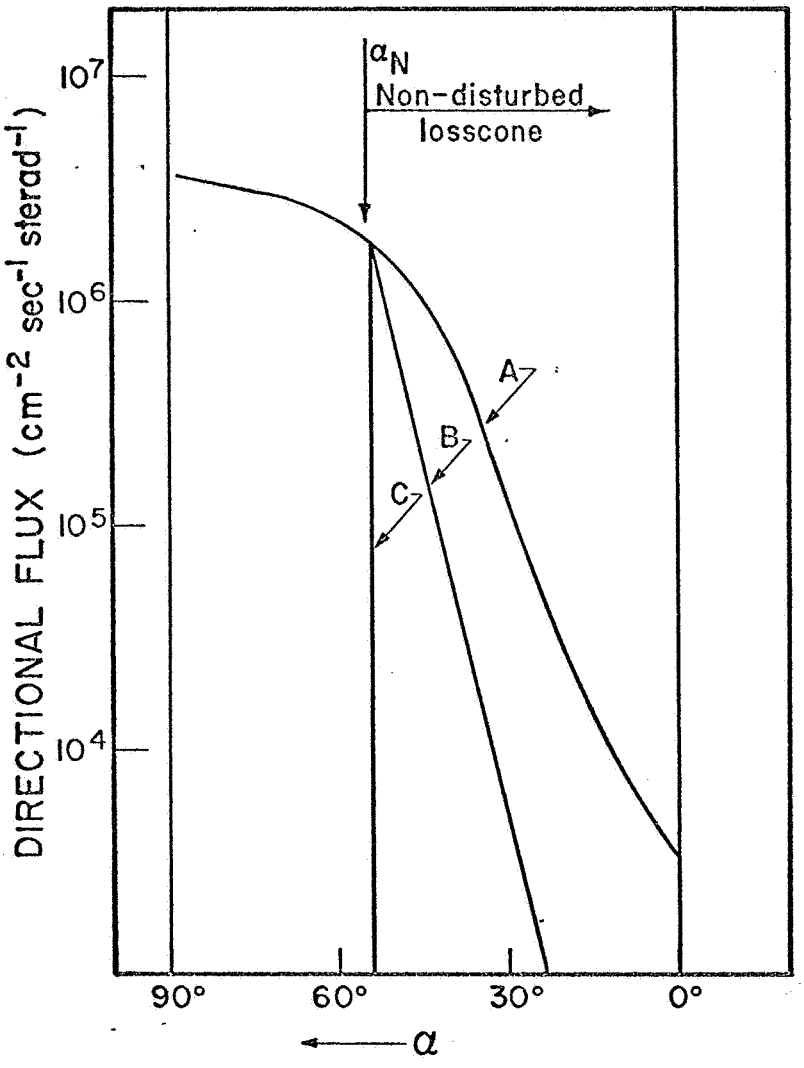
α_N
Non-disturbed
losscone
10^7
10^6
10^5
10^4
DIRECTIONAL FLUX (cm^{-2} sec^{-1} sterad^{-1})
A
B
C
90°
60°
30°
0°
α

Figure 2

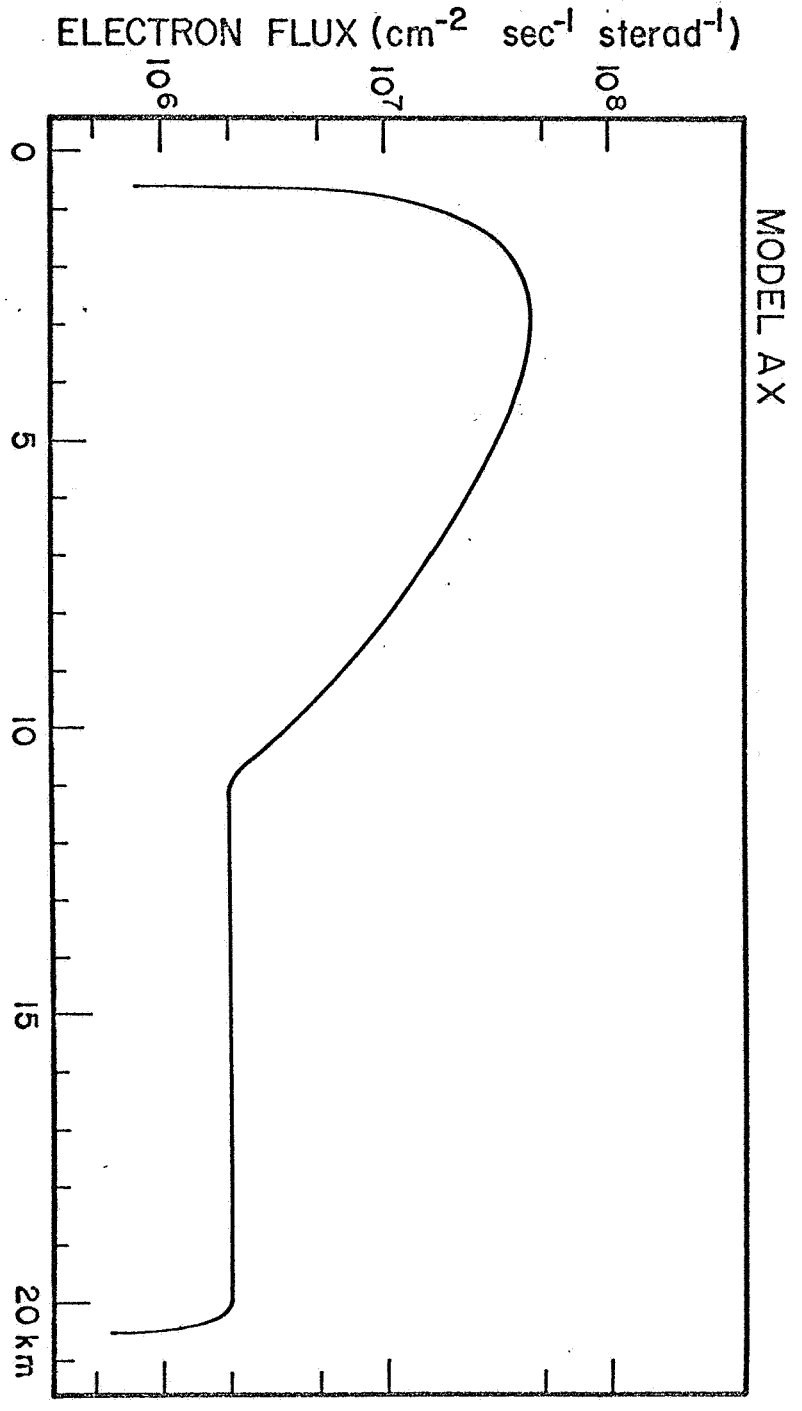

20310

Figure 3

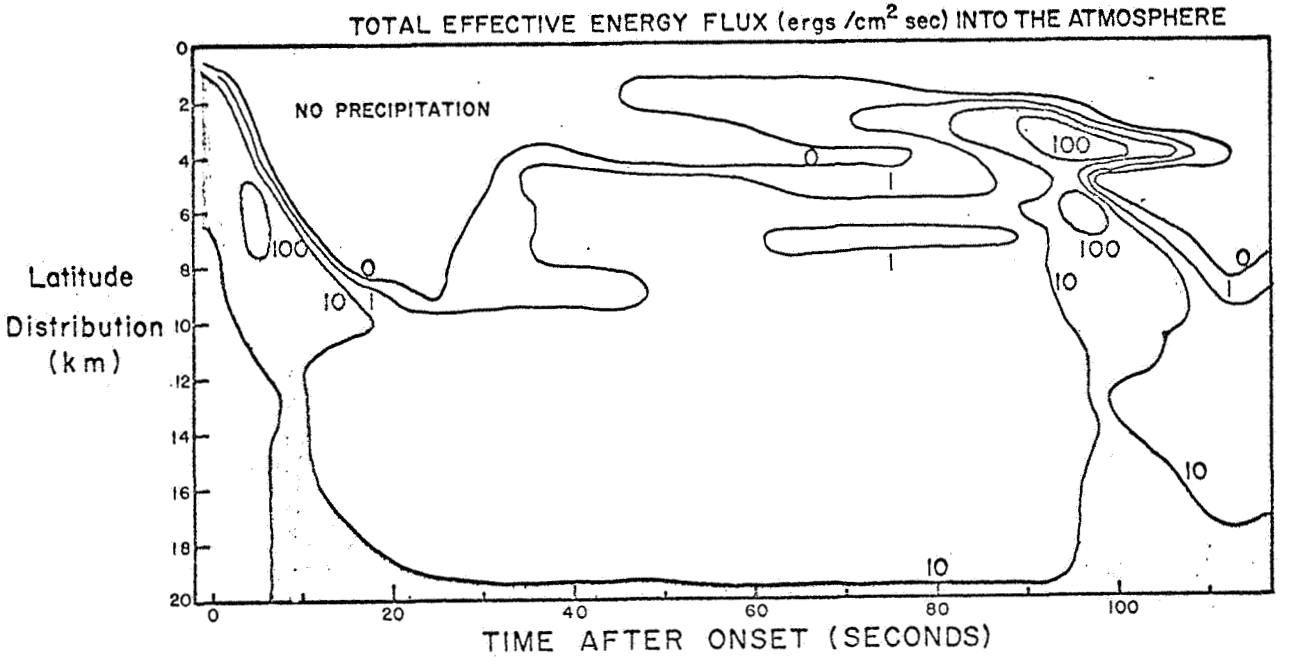
TOTAL EFFECTIVE ENERGY FLUX (ergs /cm² sec) INTO THE ATMOSPHERE
NO PRECIPITATION
Latitude Distribution (km)
TIME AFTER ONSET (SECONDS)
0
2
4
6
8
10
12
14
16
18
20
0
20
40
60
80
100
100
0
10
1
1
0
1
100
100
10
0
1
10
10

Figure 4

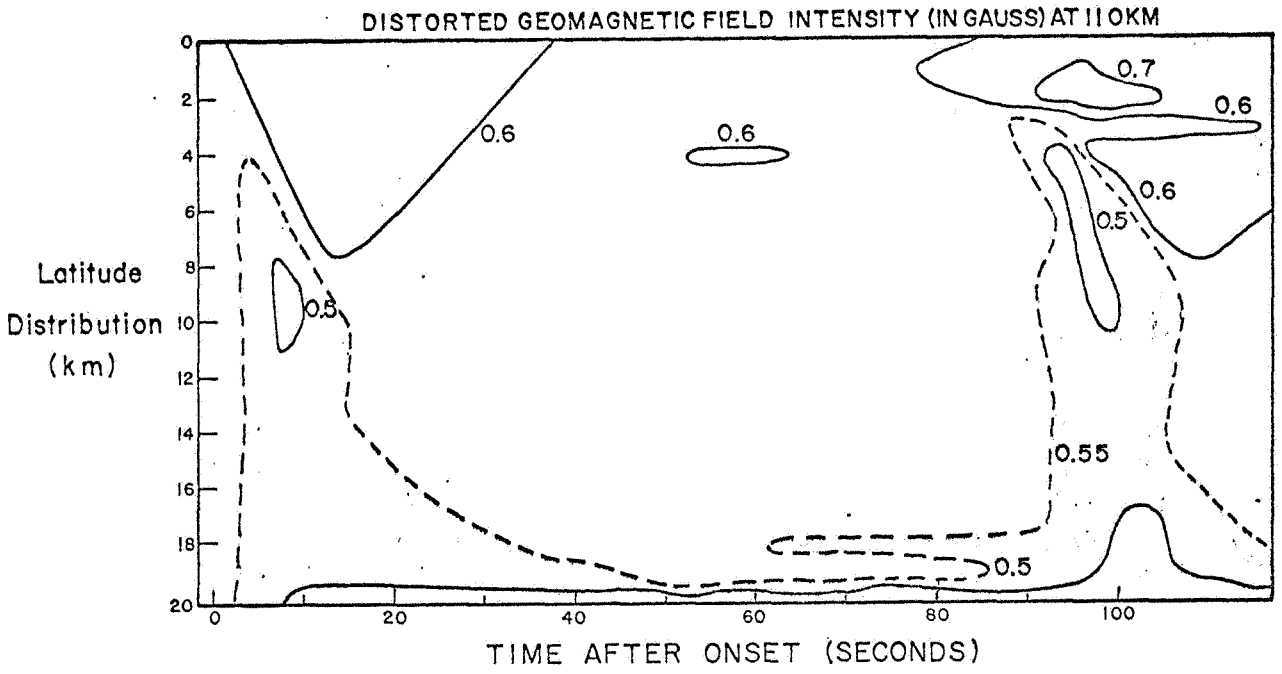
DISTORTED GEOMAGNETIC FIELD INTENSITY (IN GAUSS) AT 110KM
Latitude Distribution (km)
0
2
4
6
8
10
12
14
16
18
20
0.6
0.6
0.7
0.6
0.6
0.5
0.5
0.55
0.5
0
20
40
60
80
100
TIME AFTER ONSET (SECONDS)

Figure 5

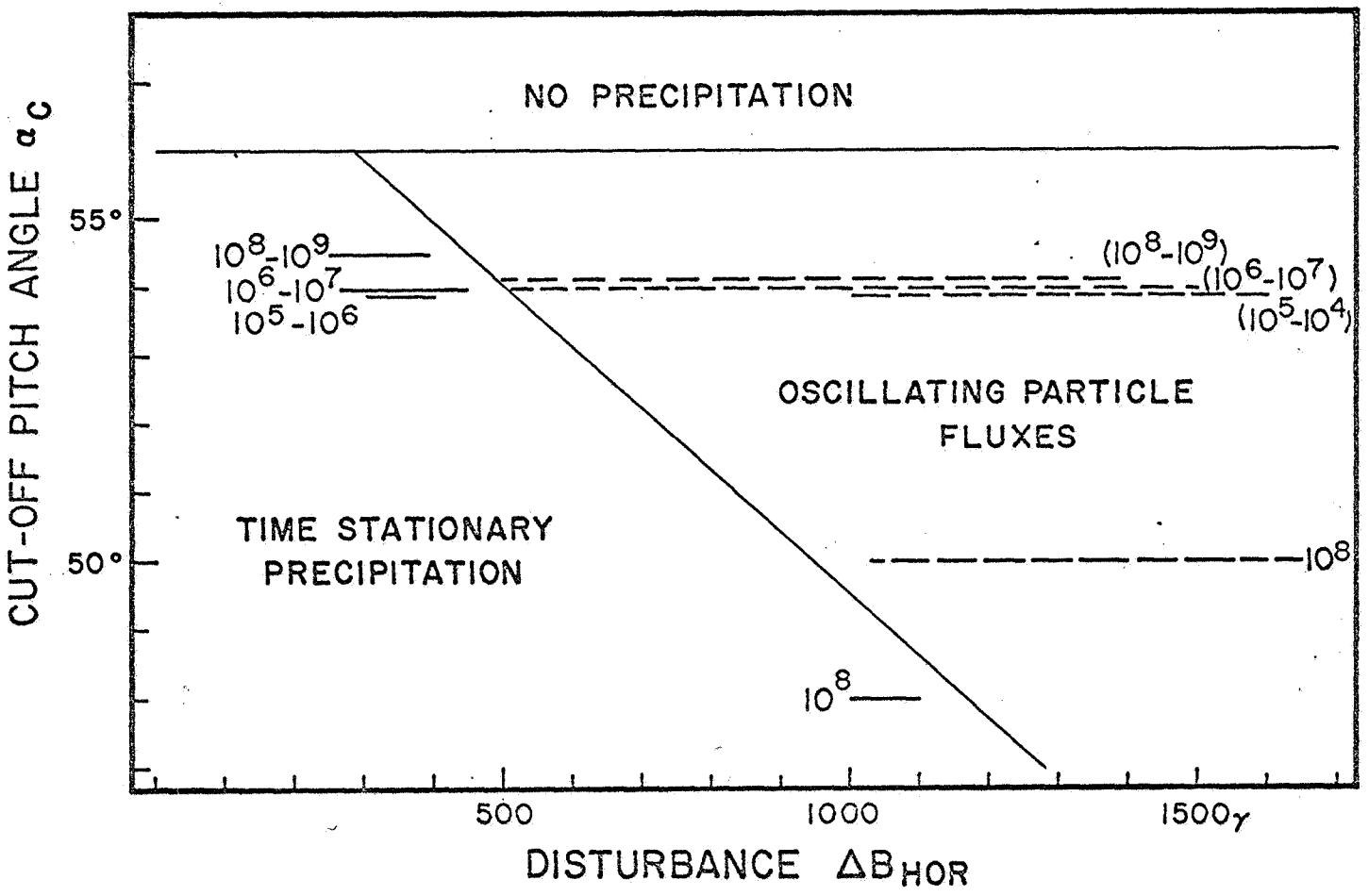
NO PRECIPITATION
55°
50°
CUT-OFF PITCH ANGLE α_c
10^8-10^9
10^6-10^7
10^5-10^6
(10^8-10^9)
(10^6-10^7)
(10^5-10^4)
OSCILLATING PARTICLE FLUXES
TIME STATIONARY PRECIPITATION
10^8
10^8
500
1000
1500γ
DISTURBANCE ΔB_{HOR}

Figure 6